processes

MDPI

Article

Comparison of the Bacterial Inactivation Efficiency of Water Activated by a Plasma Jet Source and a Pin-to-Pin Electrode Configuration Source

Radovan Čobanović [1,*], Dejan Maletić [2], Sunčica Kocić-Tanackov [1], Ivana Čabarkapa [3], Bojana Kokić [3], Predrag Kojić [1], Slobodan Milošević [4], Višnja Stulić [5], Tomislava Vukušić Pavičić [5] and Milan Vukić [6]

1 Faculty of Technology, University of Novi Sad, Bulevar cara Lazara 1, 21000 Novi Sad, Serbia; suncicat@uns.ac.rs (S.K.-T.); kojicpredrag@uns.ac.rs (P.K.)
2 Institute of Physics, University of Belgrade, Pregrevica 118, 11080 Belgrade, Serbia; dejan_maletic@ipb.ac.rs
3 Institute of Food Technology, University of Novi Sad, Bulevar cara Lazara 1, 21000 Novi Sad, Serbia; ivana.cabarkapa@fins.uns.ac.rs (I.Č.); bojana.kokic@fins.uns.ac.rs (B.K.)
4 Institute of Physics, Bijenička cesta 46, 10000 Zagreb, Croatia; slobodan@ifs.hr
5 Department of Food Engineering, Faculty of Food Technology and Biotechnology, University of Zagreb, Pierottijeva 6, 10000 Zagreb, Croatia; vstulic@pbf.hr (V.S.); tomislava.vukusic.pavicic@pbf.unizg.hr (T.V.P.)
6 Faculty of Technology Zvornik, University of East Sarajevo, Karakaj 34a, 75400 Zvornik, Bosnia and Herzegovina; milan.vukic@tfzv.ues.rs.ba
* Correspondence: radovan.cobanovic@splaboratorija.rs

Abstract: In this comparative study, the bacterial inactivation efficiency of plasma-activated water (PAW) generated by two distinct plasma reactors, one utilizing a nitrogen plasma jet electrode and the other a hybrid argon plasma reactor, was explored. The present study involved the assessment of antimicrobial activity against suspensions of three Gram-positive and three Gram-negative bacterial strains in their planktonic cell state. Bacterial suspensions were introduced into PAW five days after generation. Subsequently, the viability of the bacteria was assessed at various time intervals, specifically at 0.5, 1, 3, 5, 10, and 24 h, in order to evaluate the effect of inactivation. Structural changes in bacteria after PAW treatment were assessed using a scanning electron microscope (SEM). The physicochemical properties of PAW, including pH, conductivity, and concentrations of H_2O_2, NO_2^-, and NO_3^- during aging were measured. The present study demonstrated the effective inactivation of the tested bacterial strains by PAW. Gram-positive bacteria displayed greater resistance compared to Gram-negative species, with the lowest reductions in bacterial counts observed for *B. cereus*, and the highest for *Escherichia coli* O157:H7. Morphological damage was evident across all bacterial species examined. Physicochemical measurements showed slow decay of the reactive species in the aging process. This study illustrated the potential utility of PAW as an alternative disinfectant.

Keywords: bacteria inactivation efficiency; Gram-positive bacteria; Gram-negative bacteria; PAW; plasma activated water; plasma jet; hybrid plasma discharge; SEM imaging

Citation: Čobanović, R.; Maletić, D.; Kocić-Tanackov, S.; Čabarkapa, I.; Kokić, B.; Kojić, P.; Milošević, S.; Stulić, V.; Pavičić, T.V.; Vukić, M. Comparison of the Bacterial Inactivation Efficiency of Water Activated by a Plasma Jet Source and a Pin-to-Pin Electrode Configuration Source. *Processes* **2023**, *11*, 3286. https://doi.org/10.3390/pr11123286

Academic Editors: Tao Sun, Evgenia Benova and Frantisek Krcma

Received: 11 October 2023
Revised: 20 November 2023
Accepted: 21 November 2023
Published: 24 November 2023

1. Introduction

The threat of microbial contamination in food presents a growing concern for public health worldwide, and it has the potential to occur throughout all phases of food production and processing. The presence of spoilage microorganisms can negatively affect the nutritional value, color, texture, and edibility of food, which causes great economic losses [1], and the presence of pathogens can cause foodborne intoxication and toxicoinfections. The major etiological agents that account for the estimated 1.5 million gastrointestinal deaths each year are enterotoxigenic *Escherichia coli* (ETEC), rotavirus, *Vibrio cholerae*, and *Shigella* spp.; all are known to be endemic in the vast majority of developing countries. While standard assays can effectively identify *V. cholerae*, *Shigella*, and rotavirus, detecting ETEC poses greater challenges, which sometimes leads to its significance as a primary

cause of infantile diarrhea or cholera-like illness in individuals of all age groups going unrecognized. Additionally, it can induce traveler's diarrhea in visitors to endemic areas. Indeed, ETEC stands out as the most significant among these four pathogens in causing diarrhea in infants, children, and adults, accounting for 280 million episodes and more than 400,000 deaths annually [2]. Due to the increasing consumer preference for fresh, safe, and nutritionally enriched food products, there has been a substantial surge in research on non-thermal food processing technologies such as high hydrostatic pressure, pulsed electric fields, ultrasound, and cold plasma [3,4]. Cold plasma has attracted a lot of attention recently concerning its usage in the food and agricultural industries, mainly for applications in food sterilization and preservation [4,5]. Plasma, the fourth state of matter, is a partially ionized gas and can be generated by applying high voltage to a gas phase at low, atmospheric, and high pressures or by focused laser beams in a laboratory. There has been a growing focus on innovative approaches to pathogen inactivation, specifically those involving cold atmospheric pressure plasma (CAPP), which refers to plasma generated at atmospheric pressure and near room temperature [6]. Within the plasma, a diverse array of species is abundant, encompassing atoms and molecules in both excited and ground states, along with positive and negative ions, electrons, radicals, and high-energy photons, all characterized by substantial concentrations and fluxes [7]. CAPP has demonstrated its efficacy in surface decontamination, primarily attributed to the presence of active species known for their efficient antimicrobial properties. Nonetheless, the markedly uneven surface texture of food products provides a multitude of concealed areas where microorganisms can thrive, subsequently heightening their resilience to cold plasma treatment. Plasma-activated water (PAW) was developed to solve this problem [8]. PAW, commonly produced by exposing CAPP discharge in water or above the water surface, is an alternative disinfection method [9]. Reactive species in PAW will vary depending on the kinds of gases and liquids utilized to create it. The concentration of the major stable and long-lived reactive species (NO_3^-, NO_2^-, H_2O_2, and pH) can be easily and rapidly measured using QUANTOFIX® test strips [10]. Upon contact with water, CAPP produces a significant concentration of reactive oxygen and nitrogen species (RONS), encompassing both long-lived species like nitrate ($NO3^-$), nitrite ($NO2^-$), hydrogen peroxide (H_2O_2), and ozone (O_3), as well as short-lived species such as hydroxyl ($^{\bullet}OH$), singlet oxygen ($^1O_2$), superoxide (O_2^-), nitric oxide ($^{\bullet}NO$), and peroxynitrite ($ONOO^-$) [11,12]. The concentrations of some of these reactive species can be preserved for longer times in PAW by adding Cu metal ions originating from copper foil and nanoparticles [13]. Due to the extensive variety of RONS, PAW has a high oxidation-reduction potential (ORP) and low pH, which provides synergistic effects in the reactivity [14]. Being both environmentally friendly and economically viable, PAW demonstrates remarkable and extensive antibacterial capabilities (Figure 1). This opens up fresh avenues for its application in the realms of food production, agriculture, and the field of biomedicine [8,12,15,16].

Numerous investigations have provided evidence that PAW is highly effective in deactivating a diverse spectrum of microorganisms, encompassing fungi, viruses, bacteria, bacterial spores, and biofilms [8,12,14,16–23]. In prior studies, researchers typically employed plasma-activated water from a single specified source and applied it to a limited number of microorganisms, while the novelty of the present research is reflected in the parallel application of two different plasma sources to several pathogenic species. A significant point to note in relation to food safety is that PAW has been shown to effectively deactivate foodborne pathogens on both food-contact surfaces and food itself, all while having no adverse effects on the environment or human health [23]. Successful examples of inactivating pathogens on different food matrices include strawberries [9], fresh-cut fruits, such as pears, apples, and kiwi [24–26], and chicken meat and skin [27]. Additionally, PAW was also reported to be able to extend the shelf life of shrimp [28], baby spinach leaves [29], eggs [30], and fresh beef [31]. The enhancement of seed germination and plant growth is another potential application of PAW. Reactive species produced from chemical donors play a significant role in the germination of seeds and the development

of plants [32]. Altering the characteristics of water through non-thermal plasma and its application may influence the plant growth process, leading to improved agricultural product quality [33]. Moreover, the on-site, on-demand preparation of PAW diminishes the associated risks linked to the transportation and storage of chemicals employed in traditional sanitation procedures. Additionally, it offers a convenient and readily storable alternative to conventional disinfection solutions.

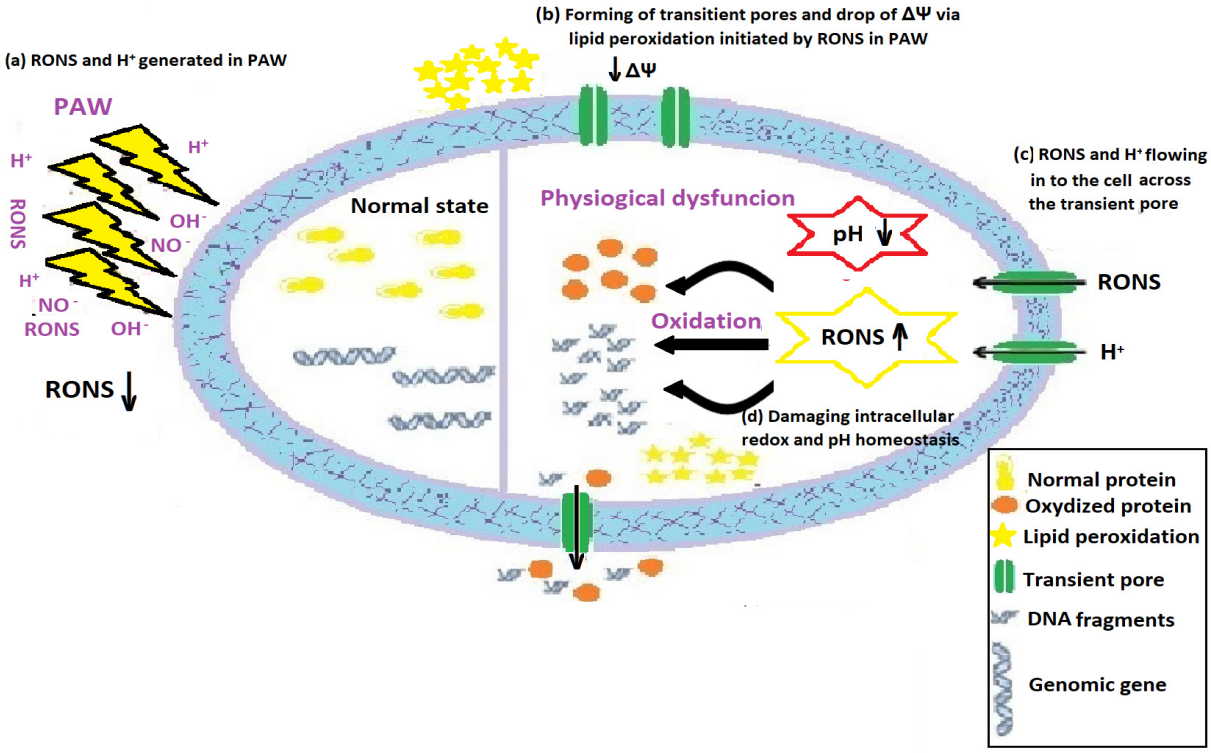

Figure 1. A schematic depiction of the plasma-induced apoptosis process that is divided into four distinct stages: (**a**) the generation of reactive oxygen and nitrogen species (RONS) within plasma-activated water (PAW) and the subsequent acidification of PAW due to plasma treatment of water; (**b**) induced cell permeabilization and disruption of the cell membrane potential caused by RONS within PAW reacting with the lipid bilayer; (**c**) the buildup of intracellular reactive oxygen species (ROS) and a reduction in intracellular pH; (**d**) DNA damage, accompanied by physiological dysfunctions resulting from the disruption of intracellular redox balance and pH homeostasis.

Despite recent advancements in PAW production technologies, several important factors still need further exploration. The effectiveness of PAW inactivation varies depending on how it is generated, and its ability to inactivate a broader range of microorganisms requires evaluation. Additionally, understanding the impact of storage stability on PAW, both in terms of its inactivation properties and physicochemical characteristics, is essential. To address these knowledge gaps, the current research focused on six representative bacterial species: *Escherichia coli* (nontoxigenic O157:H7), *Pseudomonas aeruginosa*, *Salmonella enteritidis*, *Listeria monocytogenes*, *Bacillus cereus*, and *Staphylococcus aureus*. This study investigated PAW's effectiveness in inactivating these bacteria when they are in a planktonic state. The reduction in microbial populations is described using a first-order model to explain the kinetics of microbial inactivation. Additionally, scanning electron microscope (SEM) images were taken to examine any changes in cell morphology following PAW treatment. The study also measured the concentrations of key stable reactive species (H_2O_2, NO_2^-, NO_3^-), pH, and conductivity. Furthermore, the degradation of PAW was monitored over a 40-day period.

2. Materials and Methods

2.1. Generation of Plasma-Activated Water

In this study, two types of PAW produced by two distinct plasma reactors were employed. With the first plasma reactor, an atmospheric pressure plasma jet (CAPP) [34], reactive species were produced in the plasma jet placed above the liquid surface. The second plasma reactor is a hybrid plasma reactor which combines plasma discharge in water and in the gas phase.

2.1.1. Atmospheric Pressure Plasma Jet

The plasma jet in a single-electrode configuration (Figure 2a) [35] used in this study was made of a quartz capillary with an inner diameter of 1 mm and outer diameter of 1.5 mm, as in the study by Gierczik et al. (2020) [36]. Inside the capillary, a 100 µm copper wire was placed and connected to the power supply. The capillary and the wire were both inserted into a Teflon body and connected to a gas tank via a mass flow controller (Alicat MC-5SLPM/D; Alicat Scientific, Tucson, AZ, USA). PAW was made using the 28 kHz frequency, 12 kV_{pp}, and N_2 gas (Messer 99.996% purity). The flow rate of the gas in the experiment was constant and set to 0.5 slm (standard liters per minute). The distilled water (Aqua Purificata GRAM MOL; Zagreb, Croatia) with an initial conductivity of 1.285 µS cm^{-1} and pH = 7.13 was placed below the nozzle of the plasma jet. A thin plasma channel was formed between the electrode tip and the surface of the water. The gap between the plasma jet and the water was set to 5 mm, ensuring the production of high concentrations of reactive species in PAW. A distance of 5 mm was chosen to maximize the peroxide concentration [10]. The total volume of treated water was 215 mL, and the treatment time was 40 min [37]. The total volume of the water was split into two samples, 200 mL for the bacteria treatment and 15 mL for the PAW aging measurements. To preserve the concentrations of active species in the PAW, five metal magnesium pieces (15 mm in diameter each and a total mass of 2.15 g) were placed on the bottom of the glass beaker [38]. One hour after plasma treatment, the Mg plates were removed from the PAW, and the produced PAW was stored in a fridge at 5 °C. The total input power of the plasma jet was 2.7 W and the dissipated energy was 34.8 kJ/L [36]. During the treatment, the applied voltage was monitored with an HV probe (Tektronix P6015A; Beaverton, OR, USA) and oscilloscope (Hameg-instruments, Combiscope; Mainhausen, Germany), as well as emission spectra using an Avantes spectrometer (AvaSpec-ULS-RS-TEC; Apeldoorn, The Netherlands). The label for PAW produced using the plasma jet was PAW-Jet.

2.1.2. Hybrid Plasma Reactor

A HVG60/1 PL (Impel d.o.o., Zagreb, Croatia) instrument was used for plasma treatment. The experimental setup of the hybrid plasma reactor is shown in Figure 2b. The reactor consists of a glass vessel (1000 mL) and two electrodes. The electrode configuration is the so-called pin-to-pin electrode configuration. The lower high-voltage electrode (medical needle) was placed beneath the water surface. Through the high-voltage electrode, argon gas was blowing with a flow rate of 0.5 slm, making argon bubbles in the water. The second electrode is grounded and made of stainless steel. The grounded electrode was placed above the water surface. The electrode gap between the high-voltage and grounded electrodes was 3 cm. The voltage was adjusted to 40 kV, with a frequency of 90 Hz. The input power used for treatment was 10.8 W and the total energy consumed per treatment amounted to 10.8 kJ/L [36]. The same amount of distilled water was used (215 mL) and was also split into two samples of 200 mL and 15 mL for the PAW aging measurements. The treatment time was 15 min. The label for PAW produced using the hybrid plasma was PAW-Hybrid.

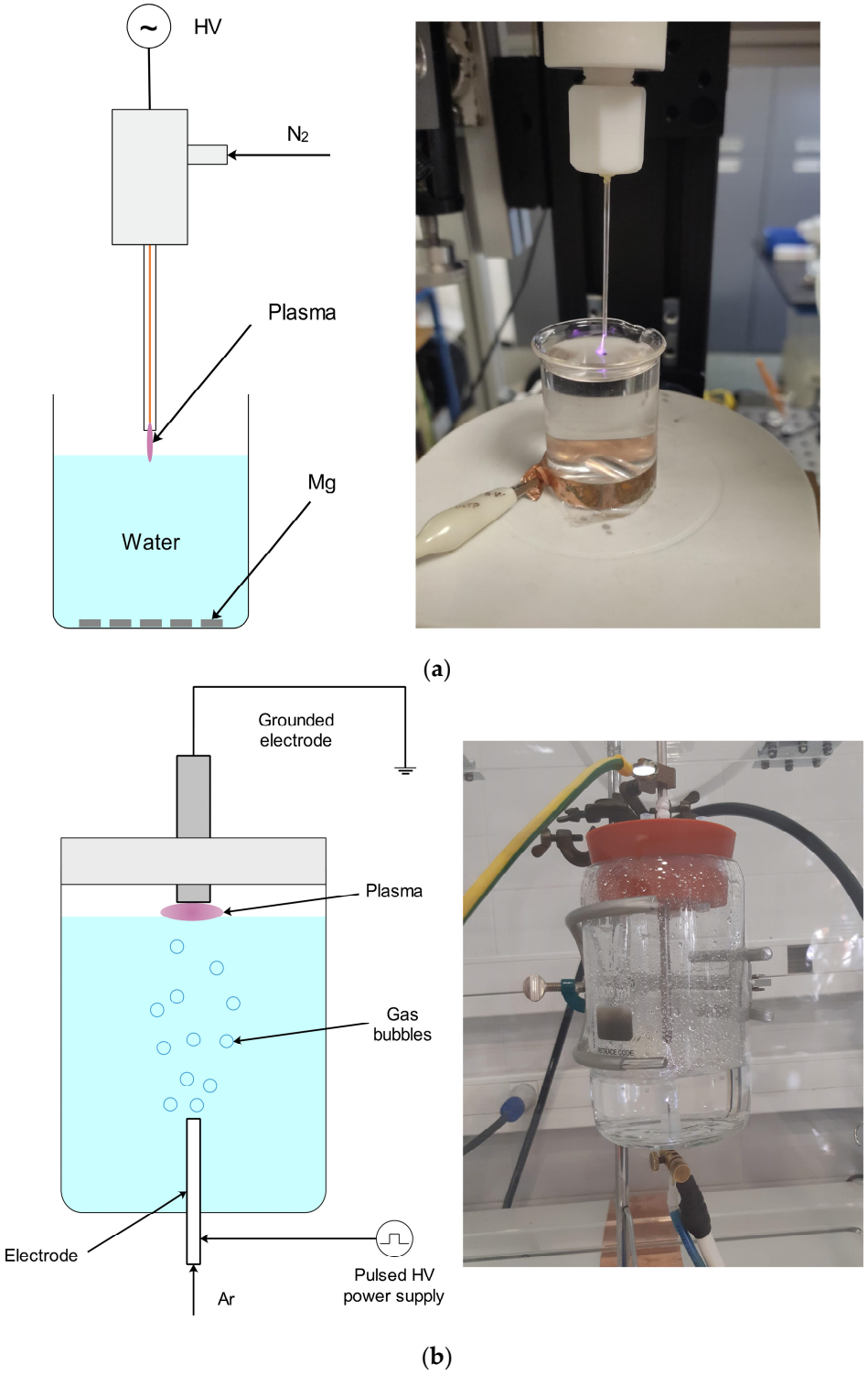

Figure 2. Schematics of the two experimental setups for PAW production: (**a**) plasma jet; (**b**) hybrid plasma reactor.

2.2. Physicochemical Properties of PAW

The reactive oxygen and nitrogen species (RONS) are generated in the gas phase and at the boundary between plasma and liquid, and captured by the liquid in the process of PAW production. The primary reactive species formed in plasma, such as hydroxyl radicals ($^{\bullet}OH$), superoxide radicals ($^{\bullet}O_2^-$), nitrate radicals ($^{\bullet}NO_3^-$), various ions (H^+, OH^+, H_3O^+, O^+, O_2^+, N^+, N_2^+, Ar^+, ArH^+), and water clusters can, through reactions, form

secondary reactive and more stable molecules, such as hydrogen peroxide (H_2O_2), ozone (O_3), and other reactive species [39–42]. The mixture of these reactive species makes PAW a highly oxidative environment that can contribute to the inactivation of microorganisms by damaging their cellular components, including lipids, proteins, and nucleic acids. The disruption of these vital components hinders the microorganisms' growth and leads to their destruction.

Plasma-activated water was characterized by determining the chemical composition, conductivity, and pH value. The majority of reactive species are created in the plasma and can interact with water, changing its physical and chemical properties. In this experiment, the concentrations of H_2O_2, NO_2^-, and NO_3^-, and the pH of the samples were measured via a semi-quantitative method (measurement accuracy $\leq$ 10%) using QUANTOFIX® test strips, and the values were read using a QUANTOFIX® Relax unit (Macherey-Nagel, Düren, Germany). With the strips and reader, we were able to measure the PAW parameters with a sufficient temporal resolution during plasma treatment for the plasma jet. We also measured the degradation of PAW in time for 40 days. Using a Metrohm 914 pH/DO/Conductometer, the pH and conductivity of the distilled water before and after treatment were measured.

Inductively coupled plasma–mass spectrometry (ICP-MS) was employed to quantitatively determine the metal ion concentrations in accordance with EPA 6020A: standard [43]. The measurements were conducted using an ICP/MS instrument (PerkinElmer, Inc., Waltham, MA, USA).

2.3. Planktonic Bacterial Suspension Preparation of Gram-Positive and Gram-Negative Bacteria

Three Gram-negative bacterial strains, *Escherichia coli* ATCC 700728 (nontoxigenic O157:H7), *Pseudomonas aeruginosa* ATCC 9027, and *Salmonella enteritidis* ATCC 13076, and three Gram-positive bacterial strains, *Listeria monocytogenes* ATCC 19112, *Bacillus cereus* ATCC 11778, *Staphylococcus aureus* ATCC 6538, were selected as the representative microorganisms. Bacterial pure culture (KWIK-STIK unit) was obtained from the strain collection of Microbiologics, Inc. (St. Cloud, MN, USA). Each KWIK-STIK unit contained a lyophilized microorganism pellet, an ampoule of hydrating fluid, and an inoculating swab and was stored at 2 to 8 °C. One inoculating swab was streaked on tryptic soy agar (TSA; Merck KGaA, Darmstadt, Germany) and incubated for 24 h to obtain isolated colonies. The incubation temperature for all six microorganisms was 35 °C. The early stationary phase of each bacterium was reached by inoculation of a single colony in tryptic soy broth and incubation at 37 °C for 18 h. The bacterial suspensions were diluted by a factor of ten in a maximum recovery diluent (MRD; Sigma-Aldrich Co. LLC, St. Louis, MO, USA) and centrifuged at 6000× *g* for 10 min. The obtained cell pellets were rinsed using sterile phosphate-buffered saline (PBS; Sigma-Aldrich Co. LLC, St. Louis, MO, USA). They were then resuspended and stored at 4 °C for later inactivation analysis, all carried out on the same day. The concentration of the bacterial suspension at the end was around 9 $\log_{10}$ CFU per mL, which was enumerated on TSA plates.

2.4. Influence of Different Exposure Times

A 1 mL aliquot of the washed bacterial suspension was introduced into 9 mL of PAW, which had been stored at 5 °C for five days. The mixture was thoroughly vortexed and then left at room temperature. To assess the influence of varying exposure durations of bacteria to PAW, time intervals of 0.5, 1, 3, 5, 10, and 24 h were chosen to measure the viable counts. For each bacterial species, a control experiment was set up in which 1 mL of the rinsed bacterial suspension was introduced into 9 mL of sterile deionized water, with no exposure to plasma treatment. These inactivation processes were individually replicated three times for each treatment.

2.5. Microbiological Analysis

To assess the effectiveness of PAW inactivation, 1 mL of treated samples was serially diluted in maximum recovery diluent (MRD; Sigma-Aldrich Co. LLC, St. Louis, MO, USA).

Using a sterile micropipette, 1 mL aliquots of appropriate dilutions were transferred to a sterile Petri dish and poured with approximately 20 mL of the tryptic soy agar (TSA; Merck KGaA, Darmstadt, Germany), previously cooled at 44 to 47 °C in a water bath. For *E. coli*, *L. monocytogenes*, *S. aureus*, *S. enteritidis*, and *P. aeruginosa*, the incubation temperature was maintained at 37 ± 1 °C, while for *B. cereus*, it was set to 30 ± 1 °C. The plates were incubated for 24 h, and the CFU was counted. The limit of detection was 1 log CFU mL^{-1}. The outcomes were presented as log_{10} colony-forming units (CFU) per milliliter (mL), and the effectiveness of PAW in inactivating microorganisms was computed using the following equation:

$$\text{Log}_{10} \text{ reduction} = \text{Log}_{10} (\text{CFU}_{\text{Control}}) - \text{Log}_{10} (\text{CFU}_{\text{Treated}}) \quad (1)$$

2.6. Scanning Electron Microscope (SEM) Imaging

The morphological changes in cell structure were examined using scanning electron microscopy analysis with and without both PAW treatments. Based on the 5 days storage of PAW, cell cultures were examined after mixing with PAW after 24 h of exposure at room temperature. Samples were prepared using the method described by Zhao et al. (2020) [20]. Following centrifugation at 6000× *g* for 10 min at 4 °C, the supernatants were removed, and the resulting cell pellets were resuspended in 500 µL of a 25% glutaraldehyde (GA) solution. To ensure proper fixation, the samples were refrigerated at 4 °C overnight. The following day, the cells were centrifuged and resuspended in PBS. This process was repeated three times to eliminate GA. Subsequently, 10 µL of the solution was dispensed onto a sterilized slide and air-dried in a fume hood for 10–15 min. These slides were then placed into 12-well plates for dehydration using a sequence of increasing ethanol concentrations (50%, 60%, 70%, 80%, 90%, and 100%). The dehydration time for ethanol concentrations between 50% and 90% was set to 5 min, while for 100% ethanol, it was 15 min. As for the drying procedure, the slides were submerged in hexamethyldisilizane (HMDS) at concentrations of 33%, 50%, 66%, and 100%, successively. Afterward, they were stored at 4 °C in a dark environment overnight before being subjected to SEM analysis. The desiccated samples were subjected to gold coating using a Sputter Coater SCD 005, BALTEC SCAN, with a working distance (WD) of 50 mm, for a duration of 90 s at a current of 30 mA. Subsequently, they were examined via scanning electron microscopy using a JMS SEM 6460 LV, operating at an acceleration voltage of 25 kV, and varying the WD from 20 to 8 mm.

2.7. PAW Microbial Inactivation Kinetics

In this investigation, the PAW microbial inactivation curves were determined by the first-order kinetics [44]. The experimental data take the shape of an exponential decay curve model and could be represented using Equation (2).

$$y(t) = y_0 e^{-k\,t} \quad (2)$$

The number of viable cells ($y(t)$) during contact time with the PAW were output values, while the only fitted coefficient (k) was the inactivation rate of the microbial population. That is the slope of the survivors' viable cells versus time for the microbial population. The coefficient y_0 represents the initial value of the microbial cells before PAW treatment, and it is fixed.

The suitability of the constructed models was assessed by employing the coefficient of determination (COD) and reduced *chi-square* (χ^2). These frequently employed parameters can be computed in the following manner:

$$chi - square = \sum_{i=1}^{N} \frac{y_{exp,i} - y_{pre,i}}{N - n} \quad (3)$$

In this equation, $y_{exp,i}$ represents the experimental values, while $y_{pre,i}$ corresponds to the predicted values derived from the model (Equation (3)) for these specific measurements. N and n denote the number of observations and the number of constants, respectively. Furthermore, a 95% predicting band interval was used to represent uncertainty and noise in the predicting model values. The relative average error between the measurements was up to 5%.

3. Results

3.1. Inactivation Efficacy of PAW

The influence of the PAW-Jet and PAW-Hybrid treatments on the microbial cells is presented in Table 1. The effectiveness of the PAW treatments was observed through Log_{10} reduction using Equation (1). A wide range of initial microbial concentrations (from 10^7 to 10^9) was used in this study (Tables 2 and 3) with the aim of investigating PAW inactivation. The inactivation kinetics were described by a first-order model and the only fitted parameter was constant rate, which shows the rate of reduction in the microbial populations. Tables 2 and 3 show that PAW treatment was most effective for *Escherichia coli* O157:H7, with k = 7.168 and k = 6.954 obtained for the hybrid plasma reactor and electrode plasma jet, respectively. On the other hand, the microbial inactivation was slowest during the PAW treatment for *Bacillus cereus*, with k = 3.072 and k = 3.792 obtained for the hybrid plasma reactor and electrode plasma jet, respectively.

Table 1. Log viable counts of the bacterial species after different exposure times with PAWs.

Bacteria	Exposure Time (h)	NT	PAW-Jet	Log_{10} Reduction	PAW-Hybrid	Log_{10} Reduction
Listeria monocytogenes	0	9.28 ± 0.01	9.28 ± 0.01	0.00	9.28 ± 0.01	0.00
	0.5		8.29 ± 0.01	0.99	8.31 ± 0.00	0.97
	1		8.21 ± 0.02	1.07	8.23 ± 0.04	1.05
	3		8.15 ± 0.02	1.13	8.10 ± 0.03	1.18
	5		8.07 ± 0.01	1.21	8.00 ± 0.01	1.28
	10		7.17 ± 0.02	2.11	6.65 ± 0.03	2.63
	24		4.09 ± 0.13	5.19	3.88 ± 0.05	5.40
Escherichia coli O157:H7	0	9.34 ± 0.04	9.34 ± 0.04	0.00	9.34 ± 0.04	0.00
	0.5		7.82 ± 0.07	1.52	7.78 ± 0.08	1.56
	1		7.81 ± 0.03	1.53	7.66 ± 0.03	1.68
	3		7.61 ± 0.03	1.73	7.45 ± 0.04	1.89
	5		7.43 ± 0.08	1.91	7.27 ± 0.03	2.07
	10		6.11 ± 0.04	3.23	6.16 ± 0.02	3.18
	24		3.54 ± 0.06	5.80	3.63 ± 0.11	5.65
Salmonella enteritidis	0	9.16 ± 0.03	9.15 ± 0.06	0.01	9.15 ± 0.06	0.01
	0.5		8.04 ± 0.02	1.12	8.01 ± 0.01	1.15
	1		7.98 ± 0.02	1.18	7.99 ± 0.02	1.17
	3		7.82 ± 0.05	1.34	7.82 ± 0.05	1.34
	5		7.66 ± 0.04	1.50	7.09 ± 0.05	2.07
	10		6.24 ± 0.03	2.92	6.14 ± 0.01	3.02
	24		4.15 ± 0.03	5.01	3.90 ± 0.04	5.26
Staphylococcus aureus	0	8.71 ± 0.03	8.71 ± 0.03	0.00	8.71 ± 0.03	0.00
	0.5		7.68 ± 0.00	1.03	7.65 ± 0.02	1.06
	1		7.52 ± 0.06	1.19	7.50 ± 0.02	1.21
	3		7.42 ± 0.06	1.29	7.40 ± 0.07	1.31
	5		7.16 ± 0.03	1.55	7.11 ± 0.02	1.60
	10		5.90 ± 0.04	2.81	6.00 ± 0.03	2.71
	24		3.67 ± 0.03	5.04	3.71 ± 0.11	5.00
Pseudomonas aeruginosa	0	8.62 ± 0.02	8.62 ± 0.03	0.00	8.62 ± 0.03	0.00
	0.5		7.44 ± 0.06	1.18	7.62 ± 0.02	1.00
	1		7.38 ± 0.08	1.24	7.49 ± 0.04	1.13
	3		7.00 ± 0.01	1.62	7.35 ± 0.04	1.27
	5		6.80 ± 0.06	1.82	6.07 ± 0.03	2.55
	10		6.26 ± 0.04	2.36	5.71 ± 0.02	2.91
	24		3.59 ± 0.05	5.03	3.55 ± 0.05	5.07
Bacillus cereus	0	7.42 ± 0.03	7.42 ± 0.03	0.00	7.42 ± 0.03	0.00
	0.5		6.55 ± 0.09	0.87	6.73 ± 0.07	0.69
	1		6.34 ± 0.02	1.08	6.31 ± 0.02	1.11
	3		6.11 ± 0.03	1.31	6.12 ± 0.02	1.30
	5		5.65 ± 0.10	1.77	5.58 ± 0.03	1.77
	10		4.52 ± 0.07	2.90	5.21 ± 0.04	2.21
	24		3.15 ± 0.08	4.27	2.80 ± 0.05	4.62

NT: non-treated (control); the results are presented as mean ± standard deviation of 3 measurements.

Table 2. Summary of kinetic coefficients with statistics, which explain the trends of the examined PAW-Jet.

PAW-Jet	*Listeria monocytogenes*	*Escherichia coli* O157:H7	*Salmonella enteritidis*	*Staphylococcus aureus*	*Pseudomonas aeruginosa*	*Bacillus cereus*
Y_0	1.92×10^9	2.28×10^9	1.40×10^9	5.27×10^8	4.18×10^8	2.68×10^7
k	-4.3 ± 0.8	-6.9 ± 0.9	-4.8 ± 0.8	-4.6 ± 0.6	-5.3 ± 0.5	-3.8 ± 0.4
Reduced Chi-Sqr	8.92×10^{15}	1.04×10^{15}	2.32×10^{15}	2.78×10^{14}	5.37×10^{13}	7.73×10^{11}
R-Square (COD)	0.98	0.99	0.99	0.99	0.99	0.99

Table 3. Summary of kinetic coefficients with statistics, which explain the trends of the examined PAW-Hybrid.

PAW-Hybrid	*Listeria monocytogenes*	*Escherichia coli* O157:H7	*Salmonella enteritidis*	*Staphylococcus aureus*	*Pseudomonas aeruginosa*	*Bacillus cereus*
Y_0	1.92×10^9	2.28×10^9	1.40×10^9	5.27×10^8	4.18×10^8	2.68×10^7
k	-4.2 ± 0.7	-7.2 ± 0.7	-4.8 ± 0.7	-4.6 ± 0.6	-4.4 ± 0.6	-3.1 ± 0.2
Reduced Chi-Sqr	7.43×10^{15}	5.17×10^{14}	2.07×10^{15}	2.78×10^{14}	2.00×10^{14}	4.44×10^{11}
R-Square (COD)	0.98	0.99	0.99	0.99	0.99	0.99

The comparison between the experimental measurements and the results calculated by the model is provided in Tables 2 and 3. The quality of the model fit was assessed, and the results of residual analysis for the developed model are presented in these tables. The one-parameter first-order mathematical model presented for predicting PAW values during the storage period is characterized as simple, robust, and accurate, with all coefficients of determination exceeding 0.981. Moreover, the mathematical models for each bacterial species exhibited no significant lack of fit, indicating that all the models effectively represented the data. The high coefficient of determination (COD) indicates that the model accounted for the variations in the data and that the data fit well with the proposed model.

3.2. Scanning Electron Microscopy Images

The effects of PAW treatment on six representative bacteria and control using SEM are shown in Figure 3. The control samples without PAW treatment had smooth and intact bacterial surfaces (Figure 3A–F). Different types of morphological changes and damage, irrespective of the PAW generation method, were observed subsequent to the treatment with PAW (Figure 3G–L; Figure 3M–R, including distortion and holes on the cell surface, deformation, rupture of the outer layer, surface roughness, and a tendency to crack.

3.3. Physicochemical Properties and Aging of PAW

pH, conductivity, and concentrations of hydrogen peroxide H_2O_2, nitrites (NO_2^-), and nitrates (NO_3^-) were monitored for 40 days from the PAW production. The PAW application on the bacteria was on the fifth day after production. The evolution of the PAW is presented in Figure 4. Non-monotonic changes in the concentration of nitrite anions, hydrogen peroxide, and pH values are a consequence of measurement accuracy $\leq 10\%$. We used Mg plates immersed in the water sample during the treatment to stabilize the concentrations of active species and prolong the antibacterial properties of the PAW. Table 4 displays the concentrations of metal ions in the water samples following plasma treatment for PAW-Jet and PAW-Hybrid. It can be seen that the concentrations of the metals for PAW-Hybrid are significantly higher than for PAW-Jet mainly because the metal electrode for the hybrid plasma reactor is immersed in water and can release metal ions during PAW production. The sources of the Mg^{2+} ions in PAW-Jet are the Mg plates that are used for PAW stabilization to prolong its efficiency. The concentration of the Mg^{2+} ions in PAW-Jet is more than three times (3.36×) higher than in the PAW-Hybrid sample.

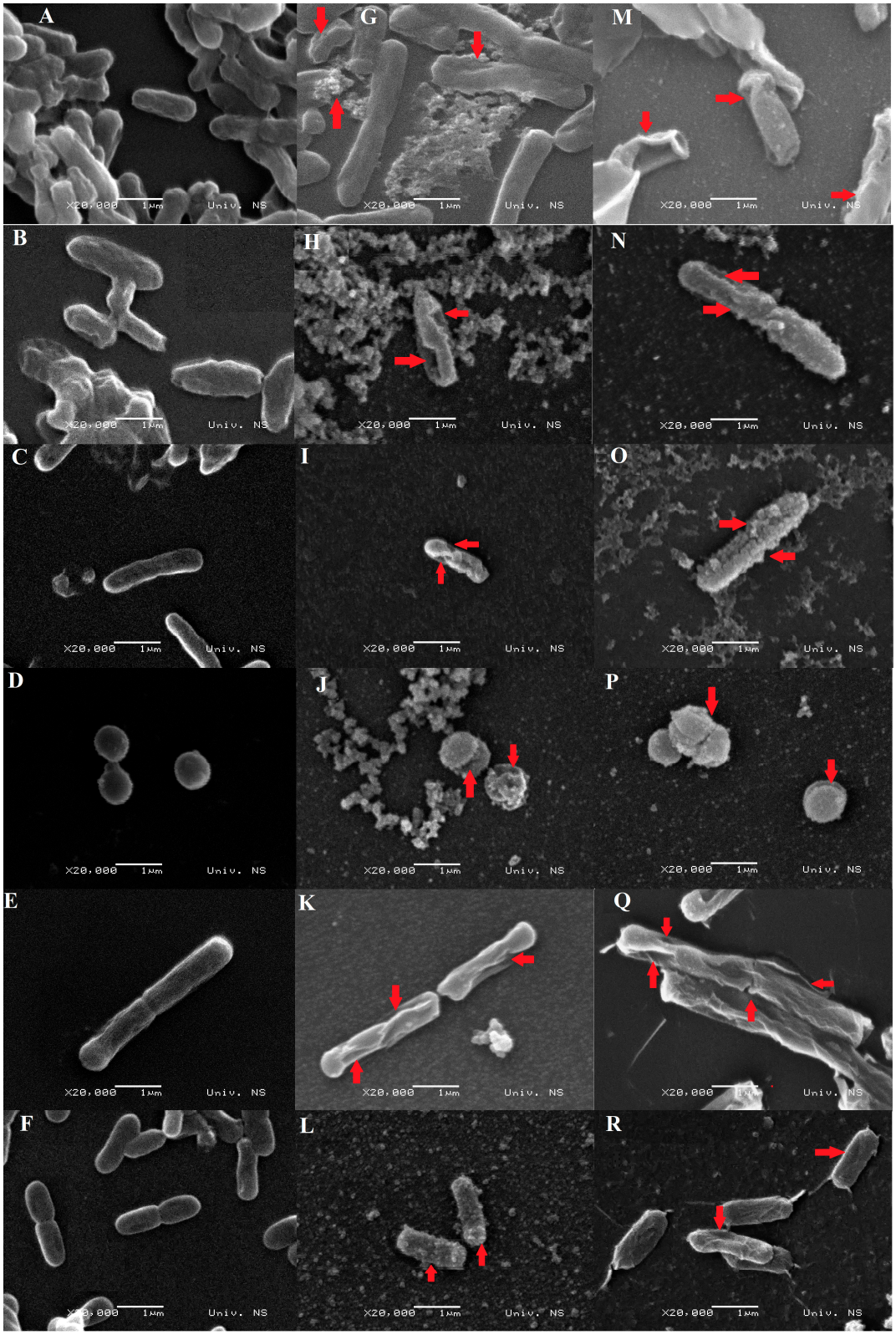

Figure 3. Scanning electron microscopy (SEM) images of the representative bacterial species from the control and both generation-method PAW treatments. (**A**–**F**) are the non-treated *Escherichia coli* (nontoxigenic O157:H7), *Salmonella enteritidis*, *Pseudomonas aeruginosa*, *Staphylococcus aureus*, *Bacillus cereus*, and *Listeria monocytogenes*, respectively; (**G**–**L**) are the corresponding bacteria treated with PAW-Jet and (**M**–**R**) are the corresponding bacteria treated with PAW-Hybrid. The damage to the cells is indicated by red arrows.

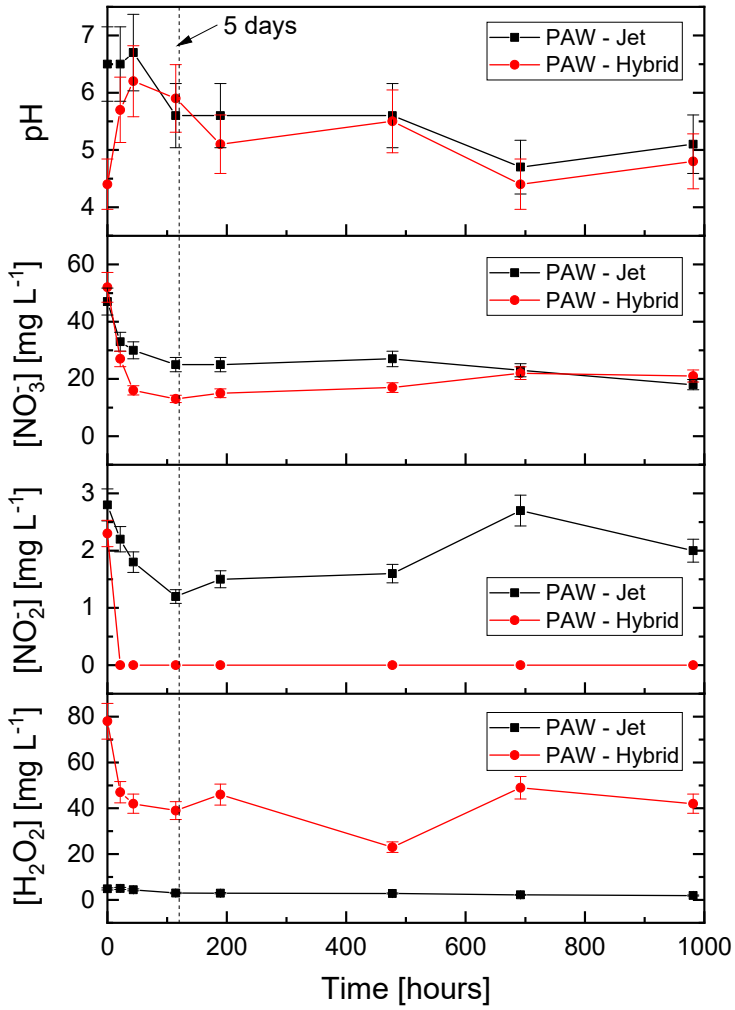

Figure 4. Aging of the PAW produced by two plasma sources, plasma jet and hybrid plasma reactor.

Table 4. The concentrations of metal ions in the water samples after plasma treatment.

Element (μg/L)	PAW-Jet	PAW-Hybrid
Ni	<1	87.9 ± 0.7
Pb	3.637 ± 0.009	4.21 ± 0.04
Fe	39.3 ± 0.9	429 ± 3
Sn	2.48 ± 0.07	1.0 ± 0.4
Na	1326 ± 7	1345 ± 12
Hg	<1	<1
Mn	<1	14.9 ± 0.4
Ca	1160 ± 34	3093 ± 13
B	10.9 ± 0.3	81.50 ± 0.06
Al	93.5 ± 0.5	30 ± 1
Se	NQ	<1
Ba	6.73 ± 0.03	8.2 ± 0.05
Mg	1882 ± 5	559 ± 4
Mo	<1	3.9 ± 0.4
As	91.2 ± 0.2	73.6 ± 0.5
K	5299 ± 4	6383 ± 32
Cr	7.28 ± 0.02	133 ± 6
Cd	<1	<1
Co	<1	2.7 ± 0.2
Zn	51.3 ± 0.3	80.0 ± 0.2
Sb	<1	<1
Cu	5.11 ± 0.09	19.9 ± 0.1
Be	<1	<1

The limit of quantification of the method is 1 μg/L; the results are presented as mean ± standard deviation of 2 measurements.

4. Discussion

The primary objective of this study was to assess the efficiency of PAW in combating six diverse bacterial species in their free-floating planktonic form. The investigation encompassed various factors, such as the use of two distinct plasma reactors, varying exposure durations, and the influence of different bacterial species on the inactivation capacity of PAW.

The findings indicated that longer plasma treatment and exposure times tended to enhance the inactivation efficacy. This was attributed to the fact that prolonged plasma treatment generated more reactive species, and longer exposure times allowed for increased interactions between these reactive species and the bacterial cells. To gain a deeper understanding of the inactivation mechanisms of PAW, SEM images of bacterial species were taken and an analysis of the physicochemical properties of PAW was conducted.

Depending on the chemical conditions, applied voltage, and the mode of generation, various reactive oxygen species (ROS) and reactive nitrogen species (RNS) may be produced. These combined ROS and RNS species, collectively referred to as RONS, are generated in plasma-activated water (PAW) and play a pivotal role in microbial inactivation. The production of these chemical species within PAW highlights the synergistic impact of high oxidation-reduction potential (ORP) and low pH, which exhibit antimicrobial properties [14]. The treatment of water with plasma caused a nonequilibrium dissociation of water molecules, resulting in the creation of short-lived species like hydroxyl ions ($OH-$) and solvated (hydrated) electrons (e_{solv}) [45,46]. The relevant reactions are as follows:

$$H_2O + e^- \rightarrow OH^\bullet + H^\bullet + e^- \quad (4)$$

$$H_2O + e^- \rightarrow OH^\bullet + H^+ + 2e^- \quad (5)$$

$$OH^\bullet + OH^\bullet \rightarrow H_2\,O_2 \quad (6)$$

$$H^\bullet + O_2 \rightarrow HO_2^\bullet \quad (7)$$

$$OH^- + H_2\,O_2 \rightarrow OOH^- + H_2O \quad (8)$$

$$*OOH \rightarrow * + O_2 + H^+ + e^- \quad (9)$$

where $*$ represents the active site of the catalyst

$$O_2 + e^- \rightarrow O^+ + O^\bullet + 2e^- \quad (10)$$

$$O_2 + O^\bullet \rightarrow O_3 \quad (11)$$

Regarding the mechanism by which ROS contribute to microbial inactivation, H_2O_2, hydroxyl ions ($^\bullet$OH), and ozone (O_3) are chemical species recognized as highly effective antimicrobial agents. It is well established that the hydroxyl radical ($^\bullet$OH) stands out as one of the most potent oxidizing agents within the category of oxygen-based oxidizers. It exhibits a notable ability to readily target unsaturated fatty acids on the cell membrane, and it can disrupt intracellular materials such as DNA [47–49]. The $^\bullet$OH radicals initiate the process of lipid peroxidation by extracting hydrogen atoms from the unsaturated carbon bonds in fatty acids, resulting in the generation of malondialdehyde (MDA) as the ultimate product [50]. MDA serves as a commonly used marker for assessing lipid oxidation. Both $^\bullet$OH and H_2O_2 possess the capability to disrupt the intramolecular bonds within peptidoglycan, potentially resulting in the breakdown of the cell wall. $^\bullet$OH achieves this by extracting a hydrogen atom from the alpha carbon of the peptide bonds (-CO-NH-) in the peptidoglycan structure, which is linked to amino acids. Additionally, it is worth noting that the transport of ROS from PAW into microbial cells can cause internal damage by breaking down DNA, and the degradation of proteins and various internal cellular components [51].

As far as the RNS mechanism of microbial inactivation is concerned, the primary influence on microbial susceptibility is the reduction in the pH in PAW. The formation of compounds like HNO_3, HNO_2, and HNOOH within PAW leads to acidification, which is responsible for microbial inactivation. Peroxynitrite ions, also formed in PAW, play a pivotal role as potent oxidizers in reactions contributing to microbial inactivation. In the presence of air, the nitrogen and oxygen from the gaseous phase undergo dissociation to generate nitrogen oxide (NO), which then interacts with water to form acidic compounds. This process leads to a decrease in pH, creating an acidic environment. The rapid decrease in pH speeds up the process of nitrite disproportionation or the breakdown of nitrite into nitrates, along with the reaction of H_2O_2 with nitrites to form $ONOO^-$s [22,52]. Some of these reactions are as follows:

$$NO_2^- + H^+ \rightarrow HNO_2 \quad (12)$$

$$NO_2^{\bullet} + OH^{\bullet} \rightarrow HNO_3 \quad (13)$$

$$2HNO_2 \rightarrow NO^{\bullet} + NO_2^{\bullet} + H_2O \quad (14)$$

$$2NO_2 + H_2O \rightarrow NO_3^- + NO_2^- + 2H^+ \quad (15)$$

$$NO_2^- + H_2O_2 + H^+ \rightarrow ONOOH + H_2O \quad (16)$$

$$ONOOH \rightarrow NO_2^{\bullet} + OH^{\bullet} \quad (17)$$

$$ONOOH \rightarrow HNO_3 \rightarrow NO_3^- + H^+ \quad (18)$$

When it comes to the resistance of the used reference strains, our findings indicated that Gram-positive bacteria exhibited greater resistance to PAW-Jet and PAW-Hybrid than Gram-negative species, with the lowest reductions observed for *B. cereus* compared with the other two Gram-positive bacteria under identical conditions. Between the other two Gram-positive bacteria examined, *S. aureus* showed much more resistance to PAW than *L. monocytogenes.* The varying responses could be partly attributed to the bacteria's morphology. An inactivation study conducted by Arroyo et al. in 1999 [53] indicated that cocci-shaped bacteria are typically more challenging to deactivate in comparison to rod-shaped bacteria. This heightened difficulty in inactivation can be attributed to the spherical shape, which results in reduced surface area in contact with the surrounding medium. Concerning the results of the reduction in Gram-negative species in both treatments, PAW-Jet and PAW-Hybrid, the least resistance was shown by *Escherichia coli* O157:H7. Other plasma inactivation studies [12,39,53–58] are in accordance with our findings. The structural variances in the bacterial cell wall are responsible for this phenomenon. The Gram-positive bacteria have a thicker cell wall, measuring between 20 and 80 nm, compared to Gram-negative bacteria, which typically have a cell wall thickness ranging from 10 to 15 nm. Consequently, this increased thickness results in greater structural rigidity and enhanced protection for bacterial cells against the reactive species formed in PAW [53].

In an attempt to explore alterations in the morphological structure of bacteria after PAW treatment, a scanning electron microscope (SEM) was employed. The SEM provided a visual confirmation of alterations in cell structure following the application of PAW treatment. In the control group, the bacterial surface appeared smooth and remained undamaged. However, following PAW treatment, various morphological changes and signs of damage were evident. All tested bacterial cells underwent a transition toward a tendency to crack. Most of the *S. enteritidis* and *P. aeruginosa* cells had holes on the cell surface and some distortion. The rupture of the outer layer was clearly seen in *B. cereus* and *E. coli*. Deformation or shrinkage was present in *S. aureus* and surface roughness in *L. monocytogenes*. Similar to our research, numerous studies have illustrated alterations in bacterial morphology through SEM images following exposure to PAW

treatment [18,20,54,56,59–61]. The images also depicted that PAW inflicted damage to the bacterial cell wall and internal structure, suggesting the potent bactericidal capabilities of PAW.

The process of PAW aging can be affected by elements such as temperature, the material of the container, and its exposure to light and air. Over time, the concentration of RONS, such as hydrogen peroxide (H_2O_2), ozone (O_3), and nitric oxide (NO), gradually decreases as these reactive species react with each other, with gas over the liquid and with the water matrix. Consequently, the oxidation-reduction potential (ORP) of PAW tends to decrease, and its pH can shift towards neutrality. As the PAW ages, it becomes less effective for certain applications that rely on high RONS concentrations. To extend the shelf life of PAW and maintain its efficacy, storage conditions and container materials are carefully considered. Dark, airtight containers at a low temperature of 5 °C are used to slow down the aging process and preserve the PAW's reactivity. Shen et al. (2016) [18] observed properties of PAW stored at different temperatures and reported that bactericidal ability increased with decreasing temperature, and that PAW should be stored at −80 °C to preserve its antibacterial characteristics. Instead of freezing PAW, we opted for the introduction of Mg discs to supply Mg^{2+} ions. This choice was made because it effectively prevents a significant drop in pH value, which in turn helps stabilize the concentration and mitigate the intense reactivity of the reactive species [62]. With this method, we have the ability to significantly prolong the lifespan of the PAW, allowing us to detect species after storing it for up to 40 days. In Figure 4, we presented the PAW aging process over a period of 40 days when stored in air flasks at a temperature of 5 °C, in a dark environment. The volume of the stored PAW was 15 mL in both cases (jet and hybrid). As we can see from the graphs, slow decay of the reactive species in the aging process is observed. The pH value before treatment was pH = 7.13; after treatment, it dropped to 6, and during the aging, the pH value was in the range from 5 to 6. The pH values for the samples without the Mg plates were slightly lower, in the range of 4–5. Changes in the pH value of the PAW are due to the dissolving of the stable molecules formed in plasma in water. The concentration of H_2O_2 is stable during the aging process. For PAW-Hybrid, the concentration of the H_2O_2 was 58 mg/mL compared to 5 mg/mL for PAW-Jet. On the day of application of the PAW, the concentrations were 42 and 3 mg/mL, respectively, for PAW-Hybrid and PAW-Jet. The concentration of nitrites is very sensitive to aging and diminishes very fast for lower pH values and higher H_2O_2 values. For example, for PAW-Hybrid, nitrites were already at zero a few hours after treatment, but for PAW-Jet, with lower starting values for H_2O_2 and larger pH values, due to the use of Mg^{2+} ions, nitrite concentrations could be preserved at about 1.5 mg/L for days. The concentrations of nitrates are similar, about 15 mg/L for both plasma reactors. Nitrates and nitrites are long-lived species that are secondary products in PAW formation. Nitrite can easily be transformed into H_2N_2 in a low-pH environment. The conductivity of the water before plasma treatment was 1.285 μS cm^{-1} and after treatment rose to 43.5 μS cm^{-1} for the hybrid plasma reactor and 31.49 μS cm^{-1} for the plasma jet. During the aging of the PAW, the conductivity increased to about 54 μS cm^{-1} after 16 days.

5. Conclusions

This study involved the selection of six representative bacterial species to assess the impact of variables such as plasma treatment time, exposure time, and bacterial species on the inactivation efficacy of PAW, with additional investigation of the bacterial inactivation mechanisms of PAW. The results demonstrated the notable antimicrobial properties of PAW, with the Gram-negative bacteria included in our study proving to be more susceptible to PAW than the Gram-positive species. Among the species examined, *B. cereus* was identified as the most resistant to PAW treatment. SEM images provided visual evidence of cell morphological damage resulting from PAW treatment. Additionally, an analysis of the physicochemical properties of PAW, including parameters such as pH, conductivity, and the presence of long-lasting reactive species like H_2O_2, NO_2^-, and NO_3^-, contributed to a more comprehensive understanding of the mechanisms involved in PAW-mediated inactivation.

Overall, this research highlights PAW as a promising disinfectant with significant potential applications within the food industry.

Author Contributions: Conceptualization, R.Č., B.K. and I.Č.; methodology, R.Č., D.M., I.Č., V.S., S.M. and T.V.P.; software, P.K. and M.V.; formal analysis, R.Č. and D.M.; investigation, R.Č., D.M., V.S., S.M. and T.V.P.; resources, R.Č., S.M., V.S. and T.V.P.; data curation, R.Č., D.M. and S.M.; writing—original draft preparation, R.Č. and D.M.; writing—review and editing, R.Č., S.K.-T., D.M., S.M., I.Č., M.V., V.S., T.V.P., P.K. and B.K.; visualization, R.Č.; supervision, S.M. All authors have read and agreed to the published version of the manuscript.

Funding: This article is based upon work from COST Action CA19110 PlAgri, supported by COST (European Cooperation in Science and Technology). This work was supported by the project Adaptation of vegetables to new agrometeorological conditions in Slavonia (AVACS), KK.05.1.1.02.0004. The project was financed by the European Union from the European Regional Development Fund. This work was also supported by the MSTDI Republic of Serbia under grant number 451-03-47/2023-01/200024 and also co-funded by the Republic of Croatia Ministry of Science and Education through the European Regional Development Fund through the project (KK.01.1.1.02.0001) "Equipping the semi-industrial practice for the development of new food technologies".

Data Availability Statement: Data are contained within the article.

Acknowledgments: The authors thank the support from the SP Laboratorija A.D. Bečej.

Conflicts of Interest: The authors declare no conflict of interest.

References

1. Amit, S.K.; Uddin, M.M.; Rahman, R.; Islam, S.M.R.; Khan, M.S. A Review on Mechanisms and Commercial Aspects of Food Preservation and Processing. *Agric. Food Secur.* **2017**, *6*, 51. [CrossRef]
2. Todd, E.C.D. Foodborne Diseases: Overview of Biological Hazards and Foodborne Diseases. In *Encyclopedia of Food Safety*; Elsevier: Amsterdam, The Netherlands, 2014; Volume 1, pp. 221–242. [CrossRef]
3. Augusto, P.E.D. Challenges, Trends and Opportunities in Food Processing. *Curr. Opin. Food Sci.* **2020**, *35*, 72–78. [CrossRef]
4. Hernández-Hernández, H.M.; Moreno-Vilet, L.; Villanueva-Rodríguez, S.J. Current Status of Emerging Food Processing Technologies in Latin America: Novel Non-Thermal Processing. *Innov. Food Sci. Emerg. Technol.* **2019**, *58*, 102233. [CrossRef]
5. Konchekov, E.M.; Gusein-zade, N.; Burmistrov, D.E.; Kolik, L.V.; Dorokhov, A.S.; Izmailov, A.Y.; Shokri, B.; Gudkov, S.V. Advancements in Plasma Agriculture: A Review of Recent Studies. *Int. J. Mol. Sci.* **2023**, *24*, 15093. [CrossRef]
6. Niemira, B.A. Cold Plasma Decontamination of Foods *. *Annu. Rev. Food Sci. Technol.* **2012**, *3*, 125–142. [CrossRef]
7. Misra, N.N.; Schlüter, O.; Cullen, P.J. Plasma in Food and Agriculture. In *Cold Plasma in Food and Agriculture: Fundamentals and Applications*; Elsevier: Amsterdam, The Netherlands, 2016; pp. 1–16. [CrossRef]
8. Thirumdas, R.; Kothakota, A.; Annapure, U.; Siliveru, K.; Blundell, R.; Gatt, R.; Valdramidis, V.P. Plasma Activated Water (PAW): Chemistry, Physico-Chemical Properties, Applications in Food and Agriculture. *Trends Food Sci. Technol.* **2018**, *77*, 21–31. [CrossRef]
9. Ma, R.; Wang, G.; Tian, Y.; Wang, K.; Zhang, J.; Fang, J. Non-Thermal Plasma-Activated Water Inactivation of Food-Borne Pathogen on Fresh Produce. *J. Hazard. Mater.* **2015**, *300*, 643–651. [CrossRef] [PubMed]
10. Kutasi, K.; Popović, D.; Krstulović, N.; Milošević, S. Tuning the Composition of Plasma-Activated Water by a Surface-Wave Microwave Discharge and a KHz Plasma Jet. *Plasma Sources Sci. Technol.* **2019**, *28*, 095010. [CrossRef]
11. Liu, Z.C.; Liu, D.X.; Chen, C.; Li, D.; Yang, A.J.; Rong, M.Z.; Chen, H.L.; Kong, M.G. Physicochemical Processes in the Indirect Interaction between Surface Air Plasma and Deionized Water. *J. Phys. D Appl. Phys.* **2015**, *48*, 495201. [CrossRef]
12. Ostrikov, K.K.; Zhou, R.; Zhou, R.; Wang, P.; Xian, Y.; Mai-Prochnow, A.; Lu, X.; Cullen, P.J.; Ostrikov, K.; Bazaka, K. Plasma-Activated Water: Generation, Origin of Reactive Species and Biological Applications. *J. Phys. D Appl. Physics.* **2020**, *53*, 303001. [CrossRef]
13. Kutasi, K.; Krstulović, N.; Jurov, A.; Salamon, K.; Popović, D.; Milošević, S. Controlling: The Composition of Plasma-Activated Water by Cu Ions. *Plasma Sources Sci. Technol.* **2021**, *30*, 045015. [CrossRef]
14. Zhang, Q.; Ma, R.; Tian, Y.; Su, B.; Wang, K.; Yu, S.; Zhang, J.; Fang, J. Sterilization Efficiency of a Novel Electrochemical Disinfectant against Staphylococcus Aureus. *Environ. Sci. Technol.* **2016**, *50*, 3184–3192. [CrossRef] [PubMed]
15. Kaushik, N.K.; Ghimire, B.; Li, Y.; Adhikari, M.; Veerana, M.; Kaushik, N.; Jha, N.; Adhikari, B.; Lee, S.J.; Masur, K.; et al. Biological and Medical Applications of Plasmaactivated. *Biol. Chem.* **2018**, *400*, 39–62. [CrossRef] [PubMed]
16. Kolb, J.F.; Mohamed, A.A.H.; Price, R.O.; Swanson, R.J.; Bowman, A.; Chiavarini, R.L.; Stacey, M.; Schoenbach, K.H. Cold Atmospheric Pressure Air Plasma Jet for Medical Applications. *Appl. Phys. Lett.* **2008**, *92*, 241501. [CrossRef]
17. Pan, J.; Sun, K.; Liang, Y.; Sun, P.; Yang, X.; Wang, J.; Zhang, J.; Zhu, W.; Fang, J.; Becker, K.H. Cold Plasma Therapy of a Tooth Root Canal Infected with Enterococcus Faecalis Biofilms in Vitro. *J. Endod.* **2013**, *39*, 105–110. [CrossRef]

18. Shen, J.; Tian, Y.; Li, Y.; Ma, R.; Zhang, Q.; Zhang, J.; Fang, J. Bactericidal Effects against S. Aureus and Physicochemical Properties of Plasma Activated Water Stored at Different Temperatures. *Sci. Rep.* **2016**, *6*, 28505. [CrossRef]
19. Wang, Q.; Salvi, D. Evaluation of Plasma-Activated Water (PAW) as a Novel Disinfectant: Effectiveness on *Escherichia coli* and *Listeria innocua*, Physicochemical Properties, and Storage Stability. *LWT* **2021**, *149*, 111847. [CrossRef]
20. Zhao, Y.M.; Ojha, S.; Burgess, C.M.; Sun, D.W.; Tiwari, B.K. Inactivation Efficacy and Mechanisms of Plasma Activated Water on Bacteria in Planktonic State. *J. Appl. Microbiol.* **2020**, *129*, 1248–1260. [CrossRef] [PubMed]
21. Guo, L.; Xu, R.; Gou, L.; Liu, Z.; Zhao, Y.; Liu, D.; Zhang, L.; Chen, H.; Kong, M.G.; Guo, C.L. Mechanism of Virus Inactivation by Cold Atmospheric-Pressure Plasma and Plasma-Activated Water. *Appl. Environ. Microbiol.* **2018**, *84*, 726–744. [CrossRef]
22. Zhao, Y.M.; Patange, A.; Sun, D.W.; Tiwari, B. Plasma-Activated Water: Physicochemical Properties, Microbial Inactivation Mechanisms, Factors Influencing Antimicrobial Effectiveness, and Applications in the Food Industry. *Compr. Rev. Food Sci. Food Saf.* **2020**, *19*, 3951–3979. [CrossRef]
23. Scholtz, V.; Pazlarova, J.; Souskova, H.; Khun, J.; Julak, J. Nonthermal Plasma—A Tool for Decontamination and Disinfection. *Biotechnol. Adv.* **2015**, *33*, 1108–1119. [CrossRef] [PubMed]
24. Chen, C.; Liu, C.; Jiang, A.; Guan, Q.; Sun, X.; Liu, S.; Hao, K.; Hu, W. The Effects of Cold Plasma-Activated Water Treatment on the Microbial Growth and Antioxidant Properties of Fresh-Cut Pears. *Food Bioproc. Tech.* **2019**, *12*, 1842–1851. [CrossRef]
25. Liu, C.; Chen, C.; Jiang, A.; Sun, X.; Guan, Q.; Hu, W. Effects of Plasma-Activated Water on Microbial Growth and Storage Quality of Fresh-Cut Apple. *Innov. Food Sci. Emerg. Technol.* **2020**, *59*, 102256. [CrossRef]
26. Zhao, Y.; Chen, R.; Liu, D.; Wang, W.; Niu, J.; Xia, Y.; Qi, Z.; Zhao, Z.; Song, Y. Effect of Nonthermal Plasma-Activated Water on Quality and Antioxidant Activity of Fresh-Cut Kiwifruit. *IEEE Trans. Plasma Sci.* **2019**, *47*, 4811–4817. [CrossRef]
27. Royintarat, T.; Choi, E.H.; Boonyawan, D.; Seesuriyachan, P.; Wattanutchariya, W. Chemical-Free and Synergistic Interaction of Ultrasound Combined with Plasma-Activated Water (PAW) to Enhance Microbial Inactivation in Chicken Meat and Skin. *Sci. Rep.* **2020**, *10*, 1559. [CrossRef]
28. Liao, X.; Su, Y.; Liu, D.; Chen, S.; Hu, Y.; Ye, X.; Wang, J.; Ding, T. Application of Atmospheric Cold Plasma-Activated Water (PAW) Ice for Preservation of Shrimps (*Metapenaeus ensis*). *Food Control* **2018**, *94*, 307–314. [CrossRef]
29. Vaka, M.R.; Sone, I.; Álvarez, R.G.; Walsh, J.L.; Prabhu, L.; Sivertsvik, M.; Fernández, E.N. Towards the Next-Generation Disinfectant: Composition, Storability and Preservation Potential of Plasma Activated Water on Baby Spinach Leaves. *Foods* **2019**, *8*, 692. [CrossRef]
30. Lin, C.M.; Chu, Y.C.; Hsiao, C.P.; Wu, J.S.; Hsieh, C.W.; Hou, C.Y. The Optimization of Plasma-Activated Water Treatments to Inactivate Salmonella Enteritidis (ATCC 13076) on Shell Eggs. *Foods* **2019**, *8*, 520. [CrossRef]
31. Zhao, Y.; Chen, R.; Tian, E.; Liu, D.; Niu, J.; Wang, W.; Qi, Z.; Xia, Y.; Song, Y.; Zhao, Z. Plasma-Activated Water Treatment of Fresh Beef: Bacterial Inactivation and Effects on Quality Attributes. *IEEE Trans. Radiat. Plasma Med. Sci.* **2020**, *4*, 113–120. [CrossRef]
32. Li, L.; Jiang, J.; Li, J.; Shen, M.; He, X.; Shao, H.; Dong, Y. Effects of Cold Plasma Treatment on Seed Germination and Seedling Growth of Soybean. *Sci. Rep.* **2014**, *4*, 5859. [CrossRef]
33. Park, D.P.; Davis, K.; Gilani, S.; Alonzo, C.A.; Dobrynin, D.; Friedman, G.; Fridman, A.; Rabinovich, A.; Fridman, G. Reactive Nitrogen Species Produced in Water by Non-Equilibrium Plasma Increase Plant Growth Rate and Nutritional Yield. *Curr. Appl. Phys.* **2013**, *13* (Suppl. 1), S19–S29. [CrossRef]
34. Zaplotnik, R.; Kregar, Z.; Bišćan, M.; Vesel, A.; Cvelbar, U.; Mozetič, M.; Milošević, S. Multiple vs. Single Harmonics AC-Driven Atmospheric Plasma Jet. *Europhys. Lett.* **2014**, *106*, 25001. [CrossRef]
35. Zaplotnik, R.; Bišćan, M.; Kregar, Z.; Cvelbar, U.; Mozetič, M.; Milošević, S. Influence of a Sample Surface on Single Electrode Atmospheric Plasma Jet Parameters. *Spectrochim. Acta Part B Spectrosc.* **2015**, *103–104*, 124–130. [CrossRef]
36. Gierczik, K.; Vukušić, T.; Kovács, L.; Székely, A.; Szalai, G.; Milošević, S.; Kocsy, G.; Kutasi, K.; Galiba, G. Plasma-Activated Water to Improve the Stress Tolerance of Barley. *Plasma Process. Polym.* **2020**, *17*, 1900123. [CrossRef]
37. Romanjek Fajdetić, N.; Benković-Lačić, T.; Mirosavljević, K.; Antunović, S.; Benković, R.; Rakić, M.; Milošević, S.; Japundžić-Palenkić, B. Influence of Seed Treated by Plasma Activated Water on the Growth of *Lactuca sativa* L. *Sustainability* **2022**, *14*, 16237. [CrossRef]
38. Kutasi, K.; Bencs, L.; Tóth, Z.; Milošević, S. The Role of Metals in the Deposition of Long-Lived Reactive Oxygen and Nitrogen Species into the Plasma-Activated Liquids. *Plasma Process. Polym.* **2023**, *20*, 2200143. [CrossRef]
39. Oehmigen, K.; Hähnel, M.; Brandenburg, R.; Wilke, C.; Weltmann, K.D.; Von Woedtke, T. The Role of Acidification for Antimicrobial Activity of Atmospheric Pressure Plasma in Liquids. *Plasma Process. Polym.* **2010**, *7*, 250–257. [CrossRef]
40. Lukes, P.; Dolezalova, E.; Sisrova, I.; Clupek, M. Aqueous-Phase Chemistry and Bactericidal Effects from an Air Discharge Plasma in Contact with Water: Evidence for the Formation of Peroxynitrite through a Pseudo-Second-Order Post-Discharge Reaction of H_2O_2 and HNO_2. *Plasma Sources Sci. Technol.* **2014**, *23*, 015019. [CrossRef]
41. Zhang, Z.; Xu, Z.; Cheng, C.; Wei, J.; Lan, Y.; Ni, G.; Sun, Q.; Qian, S.; Zhang, H.; Xia, W.; et al. Bactericidal Effects of Plasma Induced Reactive Species in Dielectric Barrier Gas–Liquid Discharge. *Plasma Chem. Plasma Process.* **2017**, *37*, 415–431. [CrossRef]
42. Hansch, M.A.C.; Mann, M.; Weltmann, K.D.; Von Woedtke, T. Analysis of Antibacterial Efficacy of Plasma-Treated Sodium Chloride Solutions. *J. Phys. D Appl. Phys.* **2015**, *48*, 454001. [CrossRef]
43. *EPA Method 6020A*; Inductively Coupled Plasma-Mass Spectrometry. U.S. EPA Office of Solid Waste (OSW) Methods Team: Washington, DC, USA, 2007.
44. Erkmen, O.; Bozoglu, T.F. *Food Microbiology: Principles into Practice*; John Wiley & Sons: West Sussex, UK, 2016; pp. 17–34.

45. Khlyustova, A.; Labay, C.; Machala, Z.; Ginebra, M.P.; Canal, C. Important Parameters in Plasma Jets for the Production of RONS in Liquids for Plasma Medicine: A Brief Review. In *Frontiers of Chemical Science and Engineering*; Higher Education Press: Beijing, China, 2019; pp. 238–252. [CrossRef]
46. Liang, Q.; Brocks, G.; Bieberle-Hütter, A. Oxygen Evolution Reaction (OER) Mechanism under Alkaline and Acidic Conditions. *J. Phys. Energy* **2021**, *3*, 026001. [CrossRef]
47. Ma, R.N.; Feng, H.Q.; Liang, Y.D.; Zhang, Q.; Tian, Y.; Su, B.; Zhang, J.; Fang, J. An Atmospheric-Pressure Cold Plasma Leads to Apoptosis in Saccharomyces Cerevisiae by Accumulating Intracellular Reactive Oxygen Species and Calcium. *J. Phys. D Appl. Phys.* **2013**, *46*, 285401. [CrossRef]
48. Kim, G.J.; Kim, W.; Kim, K.T.; Lee, J.K. DNA Damage and Mitochondria Dysfunction in Cell Apoptosis Induced by Nonthermal Air Plasma. *Appl. Phys. Lett.* **2010**, *96*, 021502. [CrossRef]
49. Zhou, R.; Zhou, R.; Zhuang, J.; Zong, Z.; Zhang, X.; Liu, D.; Bazaka, K.; Ostrikov, K. Interaction of Atmospheric-Pressure Air Microplasmas with Amino Acids as Fundamental Processes in Aqueous Solution. *PLoS ONE* **2016**, *11*, e0155584. [CrossRef]
50. Dolezalova, E.; Lukes, P. Membrane Damage and Active but Nonculturable State in Liquid Cultures of Escherichia Coli Treated with an Atmospheric Pressure Plasma Jet. *Bioelectrochemistry* **2015**, *103*, 7–14. [CrossRef]
51. Lukes, P.; Locke, B.R.; Brisset, J.-L. 7 Aqueous-Phase Chemistry of Electrical Discharge Plasma in Water and in Gas-Liquid Environments. *Plasma Chem. Catal. Gases Liq.* **2012**, *1*, 243–308.
52. Bruggeman, P.J.; Kushner, M.J.; Locke, B.R.; Gardeniers, J.G.E.; Graham, W.G.; Graves, D.B.; Hofman-Caris, R.C.H.M.; Maric, D.; Reid, J.P.; Ceriani, E.; et al. Plasma-Liquid Interactions: A Review and Roadmap. *Plasma Sources Sci. Technol.* **2016**, *25*, 053002. [CrossRef]
53. Arroyo, G.; Sanz, P.D.; Pré Stamo, G. Response to High-Pressure, Low-Temperature Treatment in Vegetables: Determination of Survival Rates of Microbial Populations Using Flow Cytometry and Detection of Peroxidase Activity Using Confocal Microscopy. *J. Appl. Microbiol.* **1999**, *86*, 544. [CrossRef]
54. Zhao, Y.M.; Ojha, S.; Burgess, C.M.; Sun, D.W.; Tiwari, B.K. Inactivation Efficacy of Plasma-Activated Water: Influence of Plasma Treatment Time, Exposure Time and Bacterial Species. *Int. J. Food Sci. Technol.* **2021**, *56*, 721–732. [CrossRef]
55. Laroussi, M.; Mendis, D.A.; Rosenberg, M. Plasma Interaction with Microbes. *New J. Phys.* **2003**, *5*, 41. [CrossRef]
56. Kamgang-Youbi, G.; Herry, J.M.; Meylheuc, T.; Brisset, J.L.; Bellon-Fontaine, M.N.; Doubla, A.; Naïtali, M. Microbial Inactivation Using Plasma-Activated Water Obtained by Gliding Electric Discharges. *Lett. Appl. Microbiol.* **2009**, *48*, 13–18. [CrossRef]
57. Ercan, U.K.; Smith, J.; Ji, H.F.; Brooks, A.D.; Joshi, S.G. Chemical Changes in Nonthermal Plasma-Treated N-Acetylcysteine (NAC) Solution and Their Contribution to Bacterial Inactivation. *Sci. Rep.* **2016**, *6*, 20365. [CrossRef]
58. Ursache, M.; Moraru, R.; Hnatiuc, E.; Nastase, V.; Mares, M. Comparative Assessment of the Relation between Energy Consumption and Bacterial Burden Reduction Using Plasma Activated Water. In Proceedings of the 2014 International Conference on Optimization of Electrical and Electronic Equipment (OPTIM), Cheile Gradistei, Romania, 22–24 May 2014; IEEE: New York, NY, USA, 2014; pp. 1036–1041. [CrossRef]
59. Liu, F.; Sun, P.; Bai, N.; Tian, Y.; Zhou, H.; Wei, S.; Zhou, Y.; Zhang, J.; Zhu, W.; Becker, K.; et al. Inactivation of Bacteria in an Aqueous Environment by a Direct-Current, Cold-Atmospheric-Pressure Air Plasma Microjet. *Plasma Process. Polym.* **2010**, *7*, 231–236. [CrossRef]
60. Ryu, Y.H.; Kim, Y.H.; Lee, J.Y.; Shim, G.B.; Uhm, H.S.; Park, G.; Choi, E.H. Effects of Background Fluid on the Efficiency of Inactivating Yeast with Non-Thermal Atmospheric Pressure Plasma. *PLoS ONE* **2013**, *8*, e66231. [CrossRef]
61. Xiang, Q.; Kang, C.; Niu, L.; Zhao, D.; Li, K.; Bai, Y. Antibacterial Activity and a Membrane Damage Mechanism of Plasma-Activated Water against Pseudomonas Deceptionensis CM2. *LWT* **2018**, *96*, 395–401. [CrossRef]
62. Vione, D.; Maurino, V.; Minero, C.; Borghesi, D.; Lucchiari, M.; Pelizzetti, E. New Processes in the Environmental Chemistry of Nitrite. 2. The Role of Hydrogen Peroxide. *Environ. Sci. Technol.* **2003**, *37*, 4635–4641. [CrossRef]